Intermedin promotes breast cancer metastasis via Src/c-Myc-mediated ribosome production and protein translation

Lingmiao Kong
Sichuan University
Fei Xiao
Sichuan University
Yong'gang Wei
Sichuan University
Zhongxue Feng
Sichuan University
Min Li
Sichuan University
Luping Huang
Sichuan University
Haili Zhang
Sichuan University
Denian Wang
Sichuan University
Hongyu Li
Sichuan University
Fei Liu
Sichuan University
Wei Zhang (zhangwei197610@163.com)
West China Hospital, Sichuan University https://orcid.org/0000-0001-7588-7249

Research article

Keywords: Breast Cancer, Metastasis, Intermedin (Adrenomedullin 2), Src, c-Myc, Ribosomal biogenesis

Posted Date: January 8th, 2021

DOI: https://doi.org/10.21203/rs.3.rs-141035/v1

Abstract

Background

Breast cancer is the most frequently diagnosed cancer and is the leading cause of cancer-associated mortality in women worldwide. Intermedin (IMD) is an endogenous peptide that belongs to the calcitonin gene-related peptide family and has been reported to play important roles in several types of cancers, including breast cancer. In this study, we sought to investigate how IMD affects the behavior of breast cancer cells, the underlying mechanism of these effects, and whether blockade of IMD has a therapeutic effect against breast cancer.

Methods

Transcriptome sequencing (RNA-Seq), cell biological experiments, Western blotting (WB), immunoprecipitation (IP), and animal tumor models were used.

Results

IMD expression was significantly increased in breast cancer samples, and the IMD level was positively correlated with lymph node metastasis and Ki67 expression. Cell biological experiments showed that IMD promoted the anchorage-independent growth, migration, and invasive ability of breast cancer cells. Inhibiting IMD activity with an anti-IMD monoclonal antibody blocked these tumor-promoting effects. In addition, blockade of IMD reduced in situ tumor growth and significantly decreased lung metastasis of 4T1 breast cancer in vivo. IMD induced Src kinase phosphorylation, which triggered the transcription of c-Myc, a major oncoprotein controlling the expression of genes that encode ribosomal components. Our data suggest that IMD is involved in breast cancer cell invasion and metastasis, potentially through increasing ribosome biogenesis and protein translation via the Src/c-Myc signaling pathway.

Conclusion

These results suggest that IMD may be a novel target for the treatment of breast cancer.

Background

Despite advances in the diagnosis and treatment of human malignancies, cancer remains one of the leading causes of morbidity and mortality worldwide. Breast cancer is currently the most frequently diagnosed cancer and is the leading cause of cancer-related mortality in women worldwide, accounting for 23% of all cancer cases diagnosed (1.38 million women) and 14% of all cancer-associated deaths (458,000 women) annually [1–3]. Metastasis is the primary cause of death in patients with breast cancer and [4]. In fact, the main cause of cancer-related death in patients with solid tumors is dissemination of

cancer cells from a primary site to form distant metastases [5]. Thus, an improved understanding of the mechanisms underlying the metastatic process and the metastatic ability of cancer cells is urgently needed.

Intermedin (IMD), also named adrenomedullin 2 (ADM2), is a member of the calcitonin family [6]. Previous studies on IMD have mainly focused on its cardiovascular functions [7–9], but the role of IMD in tumors has recently been reported [10–15]. Morimoto first reported that the expression of IMD was elevated in malignant adrenal tumors in 2008 [12]. The level of IMD in peripheral blood was found to be elevated in breast cancer and prostate cancer patients, and high IMD levels were correlated with poor survival outcomes in these patients [10, 11]. According to these findings, we hypothesized that IMD may play a role in breast occurrence or malignancy.

In this study, we evaluated the effects of IMD on the behavior of breast cancer cells, identified the mechanism underlying these effects, and determined whether blockade of IMD has a therapeutic effect on breast cancer. Herein, we report that IMD expression was significantly increased in breast cancer samples and that the expression level of IMD was positively correlated with lymph node metastasis and Ki67 expression. We found that IMD can recruit Src kinase to its receptor, calcitonin receptor-like receptor (CRLR), and induce subsequent Src phosphorylation, triggering the expression of c-Myc, which in turn initiates large-scale transcription of downstream genes, particularly genes that control ribosome biogenesis and protein translation. As a result, IMD promoted the anchorage-independent growth, migration, and invasiveness of breast cancer cells. Inhibiting IMD activity with an anti-IMD monoclonal antibody (Ab) blocked these tumor-promoting effects and significantly decreased lung metastasis in an in vivo model of 4T1 breast cancer. Our study gives novel insights into the mechanism of breast cancer metastasis and may provide a new therapeutic target for the treatment of breast cancer.

Materials And Methods

Cell Culture and Reagents

The 4T1 breast cancer cell line was obtained from ATCC and routinely cultured in complete Dulbecco's modified Eagle's medium (DMEM) supplemented with 10% fetal bovine serum at 37°C and 5% CO_2. Antibodies for CRLR (Cat. No. sc-30028) and b-actin (sc-47778) were purchased from Santa Cruz; total Src (#2108) was purchased from Cell Signaling Technology; and phospho-Src (44660G) was purchased from Invitrogen. The Src inhibitor SU6656 (Cat. S9692) was from Sigma Aldrich.

The Monoclonal Antibody to IMD

A monoclonal antibody recognizing an epitope of mouse IMD (CRPAGRRDSAPVDPSSPHSY) was generated, as described in [16]. In brief, 6 subclones (929CT5.1.1, 929CT19.2.1, 1072CT2.1.1, 1072CT2.1.2, 1106CT1.2.1, 1106CT2.2.1) that could recognize the peptide-KLH antigen were screened after immunization (ELISA assay OD 450 nm, >1/4000). The isotypes of 1072CT2.1.1 and 1072CT2.1.2 are IgG1, and 1106CT1.2.1 and 1106CT2.2.1 are IgG2b, which are appropriate subtypes to block the

activity of the target protein in a mouse model. Among them, 1106CT1.2.1 showed the highest binding capacity to mouse IMD. In addition, 1106CT1.2.1 could recognize human IMD, as evidenced by the binding capacity assay of 1106CT1.2.1 to mouse IMD and human IMD at concentrations of 1/500, 1/1000, 1/2000, 1/4000, 1/8000, 1/16000, 1/32000, 1/64000, 1/128000, and 1/256000.

Wound Healing Assay

Cells were seeded in 6-well plates and cultured until confluent. A straight scratch was made using a pipette tip at an angle of approximately 30 degrees, simulating a wound. IMD or anti-IMD was added to the medium as indicated in the figure legends. One day after scratching, the recovered area was determined by *Area 1* (before scratching) minus *Area 2* (24 h after scratching). The experiment was performed in duplicate wells and repeated three times independently.

Transwell Assay

A total of 5,000 cells were seeded in the Matrigel-coated upper chamber (Transwell inserts, pore size: 3.0 μm, Millipore) of 24-well plates and subsequently incubated at 37°C and 5% CO_2. Following incubation for 24 h, transmigrated cells on the lower surface of the membrane were stained with CFSE and fixed with 4% PFA. The total number of migrated cells was counted under a microscope. The experiment was performed in duplicate wells and repeated three times independently.

Soft Agar Formation Assay

Base Agar: 1.2% agar (molecular biology grade, low melt temperature) was melted and cooled in a 42°C water bath. Then, 2´ medium + 20% FBS + 2´ antibiotics was warmed in a 42°C water bath. At least 30 min was needed at the temperature to equilibrate. Equal volumes of the two solutions were mixed to give 0.6% agar + 1´ medium + 10% FBS + 1´ antibiotics, and the agar was allowed to set in a culture hood. Top Agar: 0.6% agar was melted and cooled in a 42°C water bath. Additionally, warm 2´ medium + 20% FBS + 2´ antibiotics was added to the same temperature. Then, 5000 cells were seeded in the 35 mm plate. The samples were incubated at 37°C prior to plating. The cells were incubated in a 37°C CO_2 incubator from 10 to 30 days, depending on cell growth.

Tumor Study

Balb/c female mice (6 weeks, 20-25 g, housed in specific pathogen-free (SPF) conditions) were used in this study. Mice were injected subcutaneously with 2.5×10^6 4T1 cells into the mammary fat pad. The tumor volume was measured every 5 days after cell injection. The tumor volume was determined by the following formula: volume (mm^3) = 1/2×length (mm)×width (mm)×width (mm). The body weights of the tumor-bearing mice were measured every 3 days accordingly. At the end point when the largest tumor reached approximately 1500 mm^3, according to the ethical standards for animal welfare, the mice were anesthetized and euthanized, and the subcutaneous tumors and the lungs were surgically removed. The metastatic colonies on the surface of the lungs were counted under a stereoscopic microscope.

Immunohistochemical (IHC) Analysis

Tumor samples (tissue chips) were fixed with 4% paraformaldehyde (PFA) for 24 hours, embedded in paraffin, and sectioned at a 3-5 μm thickness. Sections were stained with anti-IMD (1:200), and signals were developed by incubating the sections with DAB chromogen (brown) and counterstaining with hematoxylin (blue). IMD expression was scored as follows: 0 points, no positive cells; 1 point, <10% positive cells; 2 points, 10–50% positive cells; 3 points, 51–80% positive cells; and 4 points, >80% positive cells. The staining intensity was rated as follows: 1 point, weak staining; 2 points, moderate intensity; and 3 points, strong intensity. Points were added to generate overall scores. H&E staining was scored by two blinded observers.

Western Blot Analysis

Cell extracts were separated by SDS-PAGE, electrotransferred onto polyvinylidene fluoride membranes and blocked in 5% nonfat milk in Tris-buffered saline/0.01% Tween 20 for 2 h. The blots were incubated at 4°C in Tris-buffered saline with primary antibody (dilution according to the manufacturer's instructions), followed by 1 h incubation with horseradish peroxidase-conjugated secondary antibody and detection by a chemiluminescence kit (Millipore, Cat. WBKLS0100).

Immunoprecipitation (IP) Analysis

Cells were washed with ice-cold PBS and lysed with nondenaturing lysis buffer containing a proteinase inhibitor cocktail. After centrifugation, the supernatant was extracted and incubated with 2 μg antibody under continuous rotation at 4°C overnight. The mixture was then incubated with agarose beads (Cat. D00118065, Calbiochem) under continuous rotation at 4°C for 4 h. After centrifugation, the supernatant was removed. The beads were washed with nondenaturing lysis buffer, mixed with loading buffer, and then boiled for 5 min. After centrifugation, the supernatant was collected and subjected to Western blot analysis.

SiRNA Transfection

The candidate siRNAs for Src (M-040877-01-0005), β-arresin1 (M-040976-01-0005), and a scrambled nonsilencing siRNA (siR-Scram) that did not share sequence homology with any known human mRNA from a BLAST search (used as control) were purchased from Dharmacon. Transfection was performed using X-tremeGENE siRNA transfection reagent (Roche) according to the manufacturer's instructions.

Statistical Analysis

The statistical power was calculated to determine the n-number of each group. In the animal studies, no randomization was applied because all mice used in this study were genetically defined, inbred mice. When two groups for which a Gaussian distribution was assumed were compared, the unpaired, 2-tailed parametric t test with Welch's correction was used; when a Gaussian distribution was not assumed, the

unpaired, 2-tailed nonparametric Mann–Whitney U test was used. A p value < 0.05 was considered statistically significant.

Results

IMD expression is significantly increased in breast cancer samples

We first evaluated the expression level of IMD in a tissue microarray, which contained 142 breast cancer samples and 88 adjacent nontumor tissue samples (Fig. 1A and 1B). The immunohistochemical (IHC) staining results showed that the breast cancer tissues exhibited significantly increased levels of IMD expression compared with the adjacent nontumor tissues (Fig. 1C). Based on the tissue microarray data, we selected 67 paired samples (that is, tumor tissue and adjacent tissue samples from the same patient) for comparison and found that the expression of IMD in the tumor tissues of most patients was significantly higher than that in the normal tissues adjacent to the cancerous tissues (Fig. 1D). In addition, stepwise binary regression analysis showed a significant association between the IMD levels and both lymph node metastasis and Ki67 expression in the breast cancer tissues (Table 1).

IMD facilitates the malignancy of breast cancer cells

The elevated expression of IMD in breast cancer tissues suggests that it may play a role in the growth and invasion of breast cancer cells. We investigated this hypothesis using a murine breast cancer model established with 4T1 cells. The 4T1 breast cancer can produce highly metastatic solid tumors that can spontaneously metastasize to the lung, which closely mimics that of highly metastatic human breast cancer [17, 18]. The cell viability assay showed that treatment with an anti-IMD monoclonal antibody had an inhibitory effect on the growth of 4T1 cells (Fig. 2A). Anchorage-independent growth refers to the ability of cancer cells to grow independently on a solid surface and is considered a hallmark of cancer malignancy. The soft agar colony formation assay showed that IMD slightly increased the colony-forming ability of 4T1 cells, whereas the treatment with the anti-IMD antibody significantly decreased the number of cell colonies (Fig. 2B and 2C).

Cancer cell migration and invasion are highly integrated, multistep processes that play an important role in local invasion and metastasis. The wound healing assay showed that IMD promoted but the anti-IMD antibody significantly decreased the migration of 4T1 cells (Fig. 2D and 2E). The invasive ability of cancer cells, which indicates their ability to travel through the extracellular matrix into neighboring tissues, can be assessed by the Transwell assay. As shown in Fig. 2F-G, compared to the Vehicle-treated group, the number of cells crossing through the membrane in the IMD-treated group was higher; in contrast, treatment with the anti-IMD antibody significantly decreased the number of 4T1 cells that invaded into the lower chambers.

Blockade of IMD reduces in situ tumor growth and lung metastasis of 4T1 breast cancer

The elevated expression of IMD in breast cancer tissue and its effect on the malignancy of breast cancer cells suggest that blockade of IMD activity may inhibit breast cancer growth and metastasis. We tested this hypothesis in a 4T1 orthotopic breast cancer model. A total of 2.5×10^6 4T1 cells were injected under the mammary fat pads of 6-week-old female BALB/c mice. Seven days after cancer cell injection, the mice were treated with the mature IMD peptide (0.25 mg/kg/day, 2 weeks, 14 times in total, subcutaneous injection), the anti-IMD monoclonal antibody (2.5 mg/kg, twice weekly, 3 times in total, intravenous injection), or vehicle (100 ml of 0.9% saline, twice weekly, 3 times in total, intravenous injection). On the final day of the experiment, tumor growth curves were plotted (Fig. 3A). Compared with the vehicle group, IMD increased, whereas the anti-IMD antibody inhibited the orthotopic tumor growth, and the pro- or anti-tumor effects were not due to the body weight loss (Fig. 3B).

The most important feature of 4T1 tumors is not their in situ tumor growth but rather their spontaneous metastasis, particularly lung metastasis [17, 18]. Five weeks after inoculation of 4T1 cancer cells, lungs from the tumor-bearing mice in the vehicle group and the anti-IMD antibody treatment group were removed for analysis (Fig. 3C-E). Statistical analysis performed by calculating the number of metastatic colonies and the metastatic area on the surface of the lungs (including the ventral and dorsal sides) showed that anti-IMD antibody treatment reduced the number of lung metastases to approximately 1/3 of that in the vehicle group (Fig. 3F and 3G). The analysis of H&E-stained pathologic images of the whole lungs confirmed the tumor metastasis within the lungs (Fig. 4A-C). According to the results, IMD increased, whereas the anti-IMD antibody significantly inhibited lung metastasis.

Blockade of IMD significantly inhibits ribosome biogenesis and protein synthesis

To obtain a more comprehensive understanding of the influence of IMD on breast cancer cells, we analyzed the transcriptional profiles of 4T1 cells via RNA sequencing (RNA-seq) analysis. Biological replicates are necessary when performing biological experiments to ensure that the results are reliably reproducible. Herein, we analyzed two parallel samples per group (treated with vehicle, IMD, or the anti-IMD antibody). The correlation of gene expression levels between samples is an important indicator for assessing the reliability of experiments and the rationality of sample selection. The closer the correlation coefficient is to 1, the higher the similarity of the expression patterns between samples is. The Encyclopedia of DNA Elements (ENCODE) Project recommends that the square of the Pearson correlation coefficient (R^2) be greater than 0.92 (under ideal sampling and experimental conditions). Quality control (QC) analysis showed that the R^2 value of each sample was greater than 0.97, indicating good reliability of the experimental results and high similarity of expression patterns between samples (Fig. 5A).

After gene expression is quantified, statistical analysis must be performed on the expression data to screen samples for genes whose expression levels are significantly different under various treatment conditions. This analysis is generally divided into three steps [19-21]: (1) normalization of the original read counts to correct for the sequencing depth; (2) calculation of the probability value (p-value) by hypothesis testing; and (3) performance of multiple hypothesis testing and calculation of the FDR (adjusted p, or p-adj) value. A volcano plot was generated to visually show the distribution of

differentially expressed genes for each comparison (Fig. 5B and 5C). The abscissa indicates the gene expression fold change (*log2 Fold Change*) values, and the ordinate indicates the significance level of the gene expression difference (*-log10 p-adj or -log10 p-value*) between the treatment and control groups. The red dots indicate upregulated genes, and the green dots indicate downregulated genes. The volcano plot showed that IMD treatment affected gene transcriptional profiles only slightly; only 43 genes were upregulated and 41 were downregulated. The relatively small number of changed genes may be due to 4T1 cells expressing high levels of endogenous IMD; thus, supplementation with exogenous IMD may cause relatively mild effects on these cells. However, treatment with the anti-IMD antibody caused drastic changes in gene transcription; 1913 genes were significantly upregulated, and 2156 were significantly downregulated (Fig. 5C). The result suggests that inhibiting the activity of IMD may induce changes in multiple signaling pathways in breast cancer cells.

Gene Ontology (GO) analysis utilizes a comprehensive database describing gene functions that can be divided into three categories: biological processes, cellular components, and molecular functions. The most significantly enriched GO terms are displayed as scatter plots (Fig. 5D). The abscissa shows the ratio of the number of differentially expressed genes to the total number of genes in the GO term, and the ordinate shows the GO terms. The size of a dot represents the number of genes annotated to the specific GO term, and the color represents the significance of enrichment. The GO categories with significant changes (p-adj <0.05) were shown in Additional file 1. Kyoto Encyclopedia of Genes and Genomes (KEGG) analysis utilizes another database for systematic analysis of biochemical pathways, metabolic pathways, and signal transduction pathways, including differentially expressed genes. The KEGG pathway enrichment results are shown in Fig. 5E, and KEGG pathways with significant changes (p-adj <0.05) are shown in Additional file 2.

The terms with the most significant differences and the largest number of down-regulated genes were as follows: Ribonucleoprotein complex biogenesis, Ribosome biogenesis, rRNA processing, mRNA metabolic process et al. in GO terms; and Ribosome biogenesis in eukaryotes, Protein export, Spliceosome et al. in KEGG terms. Analysis of these two databases showed that anti-IMD antibody treatment had the greatest impact on ribosome biogenesis and protein synthesis.

Ribosomes are macromolecular machines that exist in almost all living cells and can perform mRNA translation and protein synthesis; they are categorized by their localization as either cytoplasmic or mitochondrial. Ribosomes consist of two major components: the small and large ribosomal subunits (S and L subunits). Each subunit consists of ribosomal RNA (rRNA) molecules and ribosomal proteins (RPs). After treatment with the anti-IMD antibody, among genes related to components of cytoplasmic ribosomes, 53 were downregulated and 6 were upregulated; among genes related to components of mitochondrial ribosomes, 25 were downregulated and only 3 were upregulated (Fig. 5F; the red box indicates gene upregulation, and the green box indicates gene downregulation; detailed differential gene expression (DEG) data are shown in Additional file 3).

IMD up-regulates the expression of ribosomal component genes by activating the Src/c-Myc signaling pathway

Cancer cells undergo uncontrolled, indefinite proliferation and persistent invasion, which requires increased production of ribosomes to support increased protein translation. The transcription of both cytoplasmic and mitochondrial ribosome components was significantly suppressed by treatment with the anti-IMD antibody, suggesting that cancer cell translation and protein production were significantly inhibited. Therefore, we sought to identify the mechanism through which IMD regulates ribosome biogenesis. KEGG pathway analysis of the “breast cancer” pathway (Fig. 6A) showed that treatment with the anti-IMD antibody suppressed the cell cycle (at the G1/S phase transition) by downregulating c-Myc and cyclin D1 (CCND1). The read count values from the original RNA-Seq data showed that IMD significantly increased the transcription levels of c-Myc and cyclin D1, whereas the anti-IMD antibody treatment significantly down-regulated the two genes (Fig. 6B-C).

c-Myc and cyclin D1 are two key genes that affect the cell cycle, cell growth and invasion. c-Myc is a major oncoprotein controlling the expression of almost 15% of all human genes, many of which are involved in ribosome biogenesis and protein translation [22]. As one of the most frequently studied oncoproteins that regulates ribosome biogenesis, c-Myc was reported to promote cell proliferation and invasion by enhancing ribosome biogenesis and protein translation largely via its key function in stimulating the transcription of numerous genes encoding proteins essential for ribosomal biogenesis [23]. As shown in Supplementary Table 3, the magnitude of the anti-IMD antibody-caused reduction in the transcription of ribosome-related genes was consistent with the magnitude of the reduction in c-Myc, which may explain the extensive inhibitory effect of the anti-IMD antibody on ribosome biogenesis-related genes.

Cyclin D1 has long been noted to play an important role in breast cancer [24]. Cyclin D1 overexpression has been reported in more than 50% of human breast cancers, and dysregulation of its expression contributes to loss of normal G1/S transition control during tumorigenesis [25]. Interestingly, Cyclin D1 was not the only cyclin-related gene affected by the anti-IMD antibody. As shown in Fig. 6D, the transcription levels of 3 genes encoding cyclin-dependent kinase inhibitors (CDKNs) were increased, whereas those of 5 genes encoding cyclin-dependent kinases (CDKs) and 8 genes encoding cyclins (D/E/G/L) were decreased. In general, CDKs and cyclins promote cell cycle progression from G1 to S phase, whereas CDKNs inhibit this process. The promotion of cell cycle progression is a major oncogenic mechanism of c-Myc, which not only activates the expression of cyclins and CDKs but also suppresses the expression of a set of proteins that act as cell cycle brakes [26]. These results indicate that c-Myc may be the key effector molecule in the IMD-regulated signaling cascade.

The activation of tyrosine kinase Src is believed to initiate expression of c-Myc for cell cycle progression in breast cancer cells [27-29]. IMD shares a G protein-coupled receptor (GPCR), CRLR (calcitonin receptor-like receptor), with its family members [6]. We have reported that IMD can induce the formation of a signaling complex containing CRLR and Src and promote subsequent Src phosphorylation in endothelial

cells [16]. Based on these results, we hypothesized that IMD may regulate the expression of c-Myc by activating Src, thereby affecting ribosome biogenesis and the cell cycle in breast cancer cells.

We tested this hypothesis using 4T1 cells. Western blot (WB) analysis showed that IMD induced a significant increase in Src phosphorylation, and this effect could be blocked by treatment with an siRNA that can specifically inhibit Src transcription (siR-Src) (Fig. 6E-G). The rescue of Src expression by transfection of Lv.Src (lentiviral vector expressing Src) restored the ability of IMD to induce Src phosphorylation (Fig. 6E-F). To determine whether the IMD-induced Src phosphorylation and c-Myc expression was causally related, we performed Real-time PCR and found that the IMD-induced c-Myc up-regulation was blocked when Src was knocked down by siR-Src (Fig. 6H). On the other hand, after Src expression was rescued by transfection of Lv.Src, the c-Myc mRNA level was restored accordingly (Fig. 6H). The results suggest that IMD up-regulates c-Myc expression via inducing Src phosphorylation.

We then asked how Src is activated by IMD. IMD has been reported to be a ligand of CRLR, a class B GPCR [6]. In our previous study, we have identified an IMD/CRLR/β-arrestin 1/Src signaling cascade in endothelial cells [16]. β-arrestin 1 is a scaffold protein that mediates the agonist-dependent recruitment of Src kinase to GPCRs [30, 31]. We have shown that in endothelial cells, after IMD binds to its receptor CRLR, with the help of β-arrestin 1, Src is recruited to CRLR and form a signaling protein complex. This Src/CRLR complex is subsequently internalized into cytoplasm, resulting in Src phosphorylation [16]. Herein, we sought to determine whether this signaling pathway exists in breast cancer cells.

We performed the immunoprecipitation (IP) assay to detect the protein interactions. We found that after exposure to IMD, the binding of Src to CRLR increased by more than 3 folds (Fig. 6I and 6J). This result suggested that IMD did promote the recruitment of Src to CRLR in 4T1 breast cancer cells. The siRNA that can specifically knockdown b-arrestin 1 transcription (siR-b-arr1) could inhibit the IMD-induced binding of Src and CRLR, and transfection of Lv.b-arr1 (lentiviral vector expressing b-arrestin 1) restored the ability of IMD to induce Src binding to CRLR (Fig. 6K-M). In addition, the IP-IB assay showed that the Src phosphorylation occurred on the Src/CRLR complex; b-arrestin 1 knockdown significantly inhibited the IMD-induced Src phosphorylation, and rescue of b-arrestin 1 expression restored the Src phosphorylation (Fig. 6N and 6O). According to these results, we may say that IMD upregulates c-Myc expression by recruiting Src to CRLR and inducing Src phosphorylation, thereby enhancing ribosome assembly and driving cell cycle progression.

Discussion

Breast cancer is the leading cause of cancer-related mortality among women worldwide and accounts for 23% of cancer diagnoses and 14% of cancer deaths annually [1-3]. Metastasis is the most important biological characteristic of malignant tumors [32-35]. In most cases, metastasis, rather than the local growth of the primary tumor, is the primary cause of death in cancer patients [33-35]. If metastasis can be effectively controlled, the treatment efficacy for cancer patients will be significantly improved. In this study, we found that IMD, an endogenous peptide belonging to the calcitonin peptide family, can recruit

and activate Src kinase to upregulate the expression of c-Myc in breast cancer cells, thereby initiating large-scale gene transcription and promoting cell cycle progression through the G1/S phase transition. Blockade of IMD inhibited the transcription of c-Myc, which decreased ribosome biogenesis and protein translation and suppressed cell cycle progression. Although the growth of primary tumors was not highly significantly inhibited, treatment with an anti-IMD antibody significantly decreased lung metastasis in an in vivo breast cancer model, suggesting that this strategy may be effective for enhancing the therapeutic effect of clinical breast cancer treatment.

Another endogenous peptide in the calcitonin peptide family in addition to IMD, adrenomedullin (Adm), has been reportedly related to the growth and metastasis of breast cancer [36-39]. Previous studies of IMD have focused mainly on its roles in mediating various cardiovascular functions [7-9], but recent studies have suggested that IMD also plays important roles in certain types of cancers, including adrenal cancer, prostate cancer, hepatocellular carcinoma, and breast cancer [10-13]. However, whether IMD affects the growth and metastasis of breast cancer is unknown, and the underlying mechanisms have not been studied. Herein, we analyzed 142 breast cancer samples and 88 adjacent tissue samples in a tissue microarray and found that compared with the normal tissues, the cancer tissues exhibited significantly increased expression of IMD and that high expression of IMD in cancer tissues was associated with an increased rate of lymph node metastasis. These findings provided evidences that IMD may play an important role in the malignancy of breast cancer cells.

Indeed, we found that IMD significantly increased the anchorage-independent growth, migration, and invasive ability of breast cancer cells. However, inhibiting IMD activity with an anti-IMD monoclonal antibody blocked these tumor-promoting effects. The elevated expression of IMD in breast cancer and its effects on the malignancy of breast cancer cells suggest that blockade of IMD activity may inhibit breast cancer growth and metastasis. We tested this hypothesis in an orthotopic breast cancer model established with 4T1 cells, which can spontaneously metastasize to the lungs. Treatment with the anti-IMD antibody not only inhibited orthotopic tumor growth but also inhibited the lung metastasis significatnly.

To provide a comprehensive understanding of gene expression profiles in breast cancer cells, we performed RNA-Seq analysis and found that the expression of both cytoplasmic and mitochondrial ribosomal components were significantly suppressed by treatment with the anti-IMD antibody. Further analysis revealed that IMD can recruit Src to its receptor CRLR and induce subsequent Src phosphorylation, triggering the expression of c-Myc, which subsequantly initiates large-scale transcription of downstream genes, particularly genes that control ribosome biogenesis and protein translation. Metastasis is a major obstacle in the treatment of breast cancers, and this process requires increased production of ribosomes to support increased protein synthesis. Thus, blockade of IMD activity with the anti-IMD antibody may be an effective strategy for inhibiting breast cancer metastasis via suppression of ribosome production and protein translation.

Taken together, our data suggest that IMD is involved in breast cancer cell metastasis by inducing increases in ribosome biogenesis and protein translation via the Src/c-Myc signaling pathway. Together with our previous finding that IMD plays a critical role in vascular remodeling and improves tumor blood perfusion [40], we may say that IMD may be a novel target for the treatment of breast cancer.

Conclusion

Our data suggest that IMD is involved in breast cancer cell invasion and metastasis, potentially by increasing ribosomal biogenesis and protein translation via the Src/c-Myc signaling cascade. These results suggest that IMD may serve as a novel target for breast cancer therapy.

Declarations

Ethics statement: The animal experiments were approved by the Animal Ethics Committee of Sichuan University and performed according to institutional and national guidelines.

Consent for publication: This manuscript has been approved by all of the authors who are properly listed and identified and by the institution where the work was carried out.

Availability of data and material: Yes.

Competing interests: There is no competing interests among the authors.

Funding: This work was supported by the National Natural Science Foundation of China (81972729 to Wei Zhang., 81971811 to Fei Xiao, and 81802095 to Hongyu Li), and Science and Technological Supports Project of Sichuan Province (2020YFS0203 to Wei Zhang, 2019YFS0372 to Yong'gang Wei, and 2019YFS0370 to Fei Liu)

Authors' contributions: LK, FX, YW, and ZF carried out the pathological analysis and cell studies; LK, FX, HL, and FL performed the animal studies; ML, LH, HZ, and DW participated in the RNA-Seq analysis; LK and FX performed the WB and IP assays; WZ conceived the initial concept and designed the study; WZ and FX draft the manuscript. All authors read and approved the final manuscript.

Acknowledgements: We thank Sisi Wu, Yu Ding, Guonian Zhu, Huifang Li, Yan Liang, Yi Zhang, and Li Zhou (Core Facilities of West China Hospital, Sichuan University) for their technical supports and helps.

References

1. Siegel RL, Miller KD, Jemal A: **Cancer Statistics, 2017**. *CA Cancer J Clin* 2017, **67**(1):7-30.
2. Siegel RL, Miller KD, Jemal A: **Cancer statistics, 2018**. *CA Cancer J Clin* 2018, **68**(1):7-30.
3. Fan L, Strasser-Weippl K, Li JJ, St Louis J, Finkelstein DM, Yu KD, Chen WQ, Shao ZM, Goss PE: **Breast cancer in China**. *Lancet Oncol* 2014, **15**(7):e279-289.

4. Redig AJ, McAllister SS: **Breast cancer as a systemic disease: a view of metastasis**. *J Intern Med* 2013, **274**(2):113-126.
5. Jacquemet G, Hamidi H, Ivaska J: **Filopodia in cell adhesion, 3D migration and cancer cell invasion**. *Curr Opin Cell Biol* 2015, **36**:23-31.
6. Roh J, Chang CL, Bhalla A, Klein C, Hsu SY: **Intermedin is a calcitonin/calcitonin gene-related peptide family peptide acting through the calcitonin receptor-like receptor/receptor activity-modifying protein receptor complexes**. *J Biol Chem* 2004, **279**(8):7264-7274.
7. Zhang JS, Hou YL, Lu WW, Ni XQ, Lin F, Yu YR, Tang CS, Qi YF: **Intermedin Protects Against Myocardial Fibrosis by Inhibiting Endoplasmic Reticulum Stress and Inflammation Induced by Homocysteine in Apolipoprotein E-Deficient Mice**. *Journal of atherosclerosis and thrombosis* 2016.
8. Hong Y, Hay DL, Quirion R, Poyner DR: **The pharmacology of adrenomedullin 2/intermedin**. *Br J Pharmacol* 2012, **166**(1):110-120.
9. Holmes D, Campbell M, Harbinson M, Bell D: **Protective effects of intermedin on cardiovascular, pulmonary and renal diseases: comparison with adrenomedullin and CGRP**. *Curr Protein Pept Sci* 2013, **14**(4):294-329.
10. Wang XL, Wang YY, He HD, Xie X, Yu ZJ, Pan YM: **Association of plasma intermedin levels with progression and metastasis in men after radical prostatectomy for localized prostatic cancer**. *Cancer biomarkers : section A of Disease markers* 2015, **15**(6):799-805.
11. Lu YM, Zhong JB, Wang HY, Yu XF, Li ZQ: **The prognostic value of intermedin in patients with breast cancer**. *Disease markers* 2015, **2015**:862158.
12. Morimoto R, Satoh F, Murakami O, Hirose T, Totsune K, Imai Y, Arai Y, Suzuki T, Sasano H, Ito S *et al*: **Expression of adrenomedullin 2/intermedin in human adrenal tumors and attached non-neoplastic adrenal tissues**. *J Endocrinol* 2008, **198**(1):175-183.
13. Guo X, Schmitz JC, Kenney BC, Uchio EM, Kulkarni S, Cha CH: **Intermedin is overexpressed in hepatocellular carcinoma and regulates cell proliferation and survival**. *Cancer Sci* 2012, **103**(8):1474-1480.
14. Shang H, Hao ZQ, Fu XB, Hua XD, Ma ZH, Ai FL, Feng ZQ, Wang K, Li WX, Li B: **Intermedin promotes hepatocellular carcinoma cell proliferation through the classical Wnt signaling pathway**. *Oncol Lett* 2018, **15**(4):5966-5970.
15. Uemura M, Yamamoto H, Takemasa I, Mimori K, Mizushima T, Ikeda M, Sekimoto M, Doki Y, Mori M: **Hypoxia-inducible Adrenomedullin in Colorectal Cancer**. *Anticancer Research* 2011, **31**(2):507-514.
16. Wang LJ, Xiao F, Kong LM, Wang DN, Li HY, Wei YG, Tan C, Zhao H, Zhang T, Cao GQ *et al*: **Intermedin Enlarges the Vascular Lumen by Inducing the Quiescent Endothelial Cell Proliferation**. *Arterioscler Thromb Vasc Biol* 2018, **38**(2):398-413.
17. Heimburg J, Yan J, Morey S, Glinskii OV, Huxley VH, Wild L, Klick R, Roy R, Glinsky VV, Rittenhouse-Olson K: **Inhibition of spontaneous breast cancer metastasis by anti-Thomsen-Friedenreich antigen monoclonal antibody JAA-F11**. *Neoplasia* 2006, **8**(11):939-948.

18. Pulaski BA, Ostrand-Rosenberg S: **Reduction of established spontaneous mammary carcinoma metastases following immunotherapy with major histocompatibility complex class II and B7.1 cell-based tumor vaccines**. *Cancer Res* 1998, **58**(7):1486-1493.
19. Anders S, Huber W: **Differential expression analysis for sequence count data**. *Genome Biol* 2010, **11**(10):R106.
20. Love MI, Huber W, Anders S: **Moderated estimation of fold change and dispersion for RNA-seq data with DESeq2**. *Genome Biol* 2014, **15**(12):550.
21. Robinson MD, McCarthy DJ, Smyth GK: **edgeR: a Bioconductor package for differential expression analysis of digital gene expression data**. *Bioinformatics* 2010, **26**(1):139-140.
22. Patel JH, Loboda AP, Showe MK, Showe LC, McMahon SB: **Analysis of genomic targets reveals complex functions of MYC**. *Nat Rev Cancer* 2004, **4**(7):562-568.
23. Oskarsson T, Trumpp A: **The Myc trilogy: lord of RNA polymerases**. *Nat Cell Biol* 2005, **7**(3):215-217.
24. Barnes DM, Gillett CE: **Cyclin D1 in breast cancer**. *Breast Cancer Res Treat* 1998, **52**(1-3):1-15.
25. Velasco-Velazquez MA, Li Z, Casimiro M, Loro E, Homsi N, Pestell RG: **Examining the role of cyclin D1 in breast cancer**. *Future Oncol* 2011, **7**(6):753-765.
26. Garcia-Gutierrez L, Delgado MD, Leon J: **MYC Oncogene Contributions to Release of Cell Cycle Brakes**. *Genes (Basel)* 2019, **10**(3).
27. Barone MV, Courtneidge SA: **Myc but not Fos rescue of PDGF signalling block caused by kinase-inactive Src**. *Nature* 1995, **378**(6556):509-512.
28. Bromann PA, Korkaya H, Webb CP, Miller J, Calvin TL, Courtneidge SA: **Platelet-derived growth factor stimulates Src-dependent mRNA stabilization of specific early genes in fibroblasts**. *J Biol Chem* 2005, **280**(11):10253-10263.
29. Abdullah C, Korkaya H, Iizuka S, Courtneidge SA: **SRC Increases MYC mRNA Expression in Estrogen Receptor-Positive Breast Cancer via mRNA Stabilization and Inhibition of p53 Function**. *Molecular and cellular biology* 2018, **38**(6).
30. Lefkowitz RJ, Shenoy SK: **Transduction of receptor signals by beta-arrestins**. *Science* 2005, **308**(5721):512-517.
31. Luttrell LM, Ferguson SS, Daaka Y, Miller WE, Maudsley S, Della Rocca GJ, Lin F, Kawakatsu H, Owada K, Luttrell DK *et al*: **Beta-arrestin-dependent formation of beta2 adrenergic receptor-Src protein kinase complexes**. *Science* 1999, **283**(5402):655-661.
32. McAllister SS, Weinberg RA: **The tumour-induced systemic environment as a critical regulator of cancer progression and metastasis**. *Nat Cell Biol* 2014, **16**(8):717-727.
33. Bottos A, Hynes NE: **Cancer: Staying together on the road to metastasis**. *Nature* 2014, **514**(7522):309-310.
34. Valastyan S, Weinberg RA: **Tumor metastasis: molecular insights and evolving paradigms**. *Cell* 2011, **147**(2):275-292.
35. Hanahan D, Weinberg RA: **Hallmarks of cancer: the next generation**. *Cell* 2011, **144**(5):646-674.

36. Liu LL, Chen SL, Huang YH, Yang X, Wang CH, He JH, Yun JP, Luo RZ: **Adrenomedullin inhibits tumor metastasis and is associated with good prognosis in triple-negative breast cancer patients**. *Am J Transl Res* 2020, **12**(3):773-786.
37. Siclari VA, Mohammad KS, Tompkins DR, Davis H, McKenna CR, Peng X, Wessner LL, Niewolna M, Guise TA, Suvannasankha A *et al*: **Tumor-expressed adrenomedullin accelerates breast cancer bone metastasis**. *Breast Cancer Res* 2014, **16**(6):458.
38. Oehler MK, Fischer DC, Orlowska-Volk M, Herrle F, Kieback DG, Rees MC, Bicknell R: **Tissue and plasma expression of the angiogenic peptide adrenomedullin in breast cancer**. *Br J Cancer* 2003, **89**(10):1927-1933.
39. Martinez A, Vos M, Guedez L, Kaur G, Chen Z, Garayoa M, Pio R, Moody T, Stetler-Stevenson WG, Kleinman HK *et al*: **The effects of adrenomedullin overexpression in breast tumor cells**. *J Natl Cancer Inst* 2002, **94**(16):1226-1237.
40. Zhang W, Wang LJ, Xiao F, Wei Y, Ke W, Xin HB: **Intermedin: a novel regulator for vascular remodeling and tumor vessel normalization by regulating vascular endothelial-cadherin and extracellular signal-regulated kinase**. *Arterioscler Thromb Vasc Biol* 2012, **32**(11):2721-2732.

Tables

Stepwise binary logic regression analysis(IMD score ≤5 / IMD score>5)							
		B	S.E	Wald	df	Sig.	Exp(B)
step 1[a]	Age	0.020	0.018	1.207	1	0.272	1.020
	Tumor volume	-0.001	0.004	0.058	1	0.810	0.999
	Clinical stage	0.497	0.512	0.943	1	0.332	1.644
	LNM	-2.191	1.065	4.234	1	0.040*	0.112
	ER	-0.101	0.767	0.017	1	0.895	0.904
	PR	0.271	0.831	0.106	1	0.744	1.311
	HER2	-0.245	0.730	0.112	1	0.738	0.783
	Ki67	3.202	1.222	6.871	1	0.009**	24.589
	Constant	-3.430	1.567	4.793	1	0.029*	0.032
a. variable(s) entered on step 1：Age, Tumor volume, Clinical stage, LNM, ER, PR, HER2, Ki67							
IMD: intermedin; LNM: Lymph nodes metastasis; ER: estrogen receptor; PR: progesterone receptor; Her-2: Her2-receptor.							

Figures

Figure 1

IMD expression is significantly increased in breast cancer samples. A-B, IHC images of non-tumor tissues and breast cancer samples. C, The IMD staining scores were presented as columns with mean ± SD. Significance was assessed by unpaired t test with Welch's correction. D, The IMD staining scores of 67 one-to-one samples (a sample from a breast cancer tissue and the adjacent non-tumor tissue from the same patient).

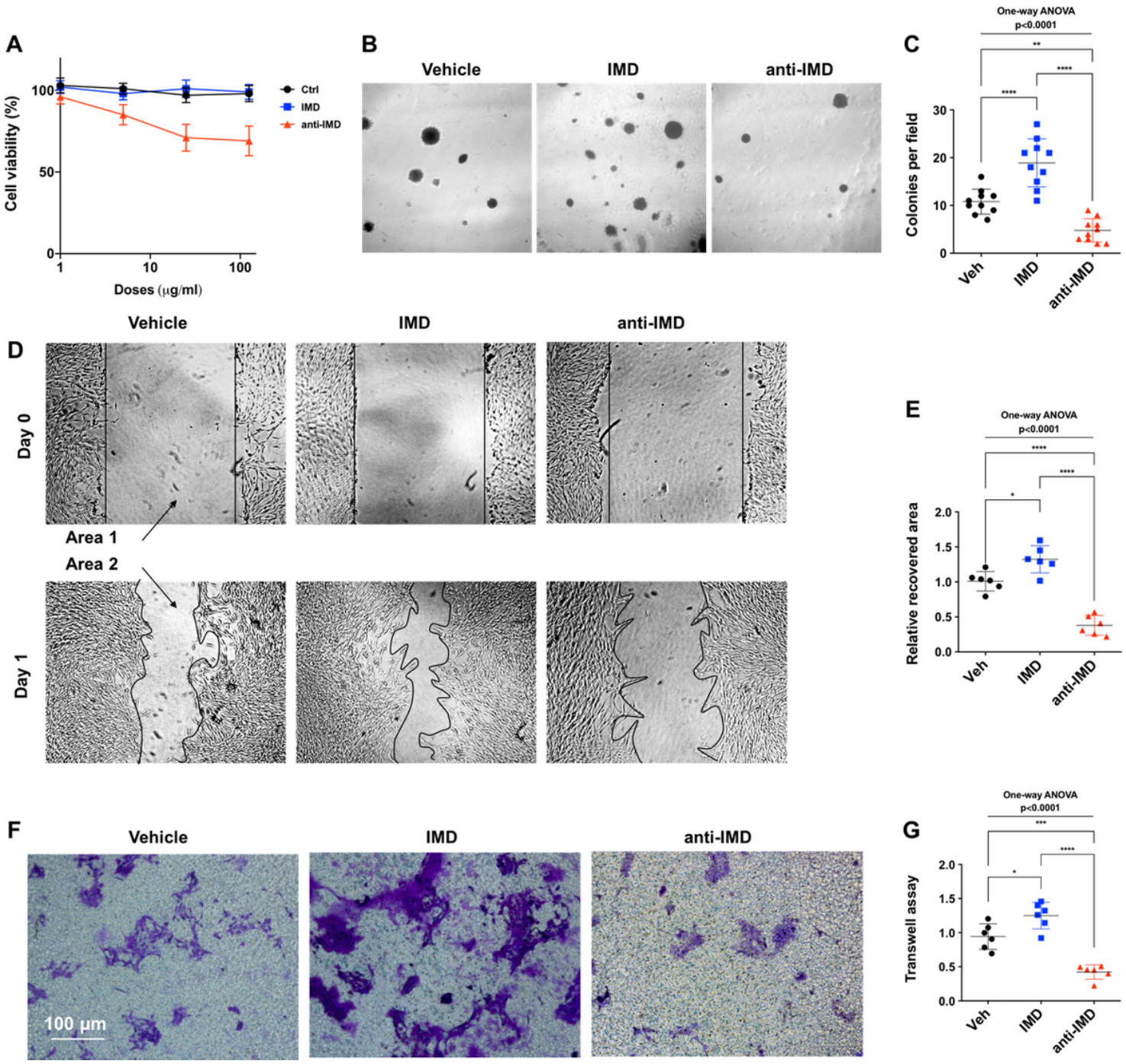

Figure 2

IMD facilitates malignancy of breast cancer cells. A, 4T1 cells were treated with IMD (2.5μg/ml), anti-IMD antibody (25μg/ml), or vehicle, and the cell viability was measured. Data were presented as scatter plots with mean ± SD (n=6). B, 4T1 cells treated with IMD, anti-IMD, or vehicle were subjected to Soft agar formation assay. C, Cell colonies were quantified using 10 randomly chosen fields. D, Cells were seeded on the 6-well plates. One day after cell scratching, the recovered area was measured by Area 1 (the area that had not been covered by cells at Day 0) minus Area 2 (the area that was not covered by cells at Day 1)." E: The recovered area (the mean level of the control group was set to 1) was calculated (n=6). F: Cells were seeded on the upper chamber of the transwell system. Representative images demonstrated the

Crystal-violet-stained cells that invaded through the membranes. G: The Crystal-violet-positive cells was calculated (relative to the control; the mean level in the control group was set to 1.0; n=6.). All data were presented as scatter plots with mean ± SD. Significance was assessed by one-way ANOVA followed by non-parametric Dunn's post-hoc analysis.

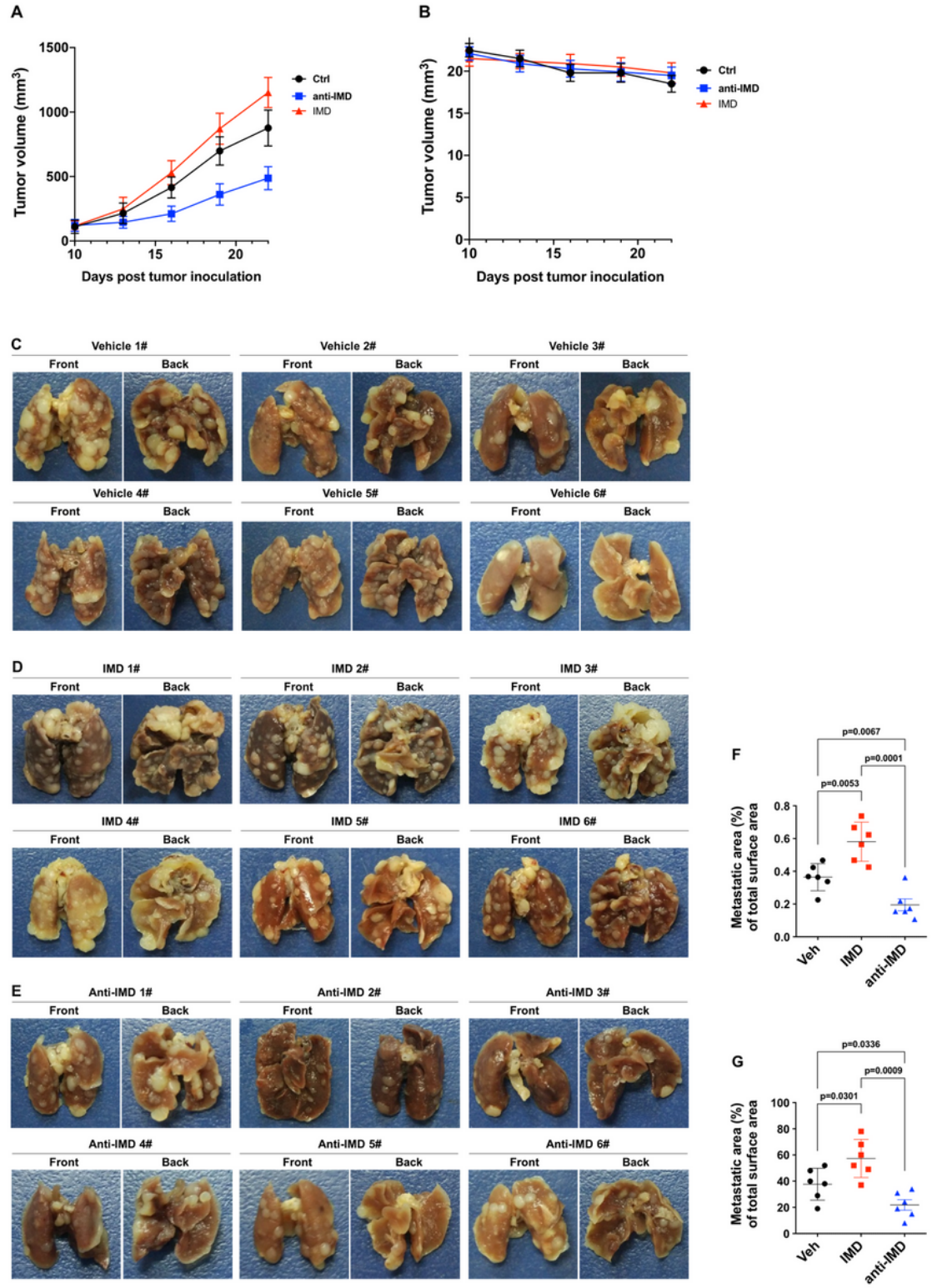

Figure 3

Blockade of IMD reduced the growth and metastasis of 4T1 tumor. A, 2.5×106 4T1 cells were injected into the mammary fat pad of mice. Seven days after tumor inoculation. Seven days after tumor inoculation, the mature IMD peptide (0.25 mg/kg/day, 2 weeks, 14 times in total, subcutaneous injection), or the anti-IMD monoclonal antibody (2.5 mg/kg, twice weekly, 3 times in total, intravenous injection), or vehicle (100 μl of 0.9% saline, twice weekly, 3 times in total, intravenous injection) were administrated. The tumor volumes were measured every 5 days until the biggest tumor reaches approximately 1,500 mm3. B, Body weight of the tumor-bearing mice were measured every 3 days. C-E, Pictures of the lungs (front side and back side) from the 4T1 tumor-bearing mice were shown. F and G, Number of metastatic colonies and the metastatic area (%) of total surface area of the lungs were calculated. Data were presented as scatter plots with mean ± SD. Significance was assessed by unpaired t test with Welch's correction (n=6).

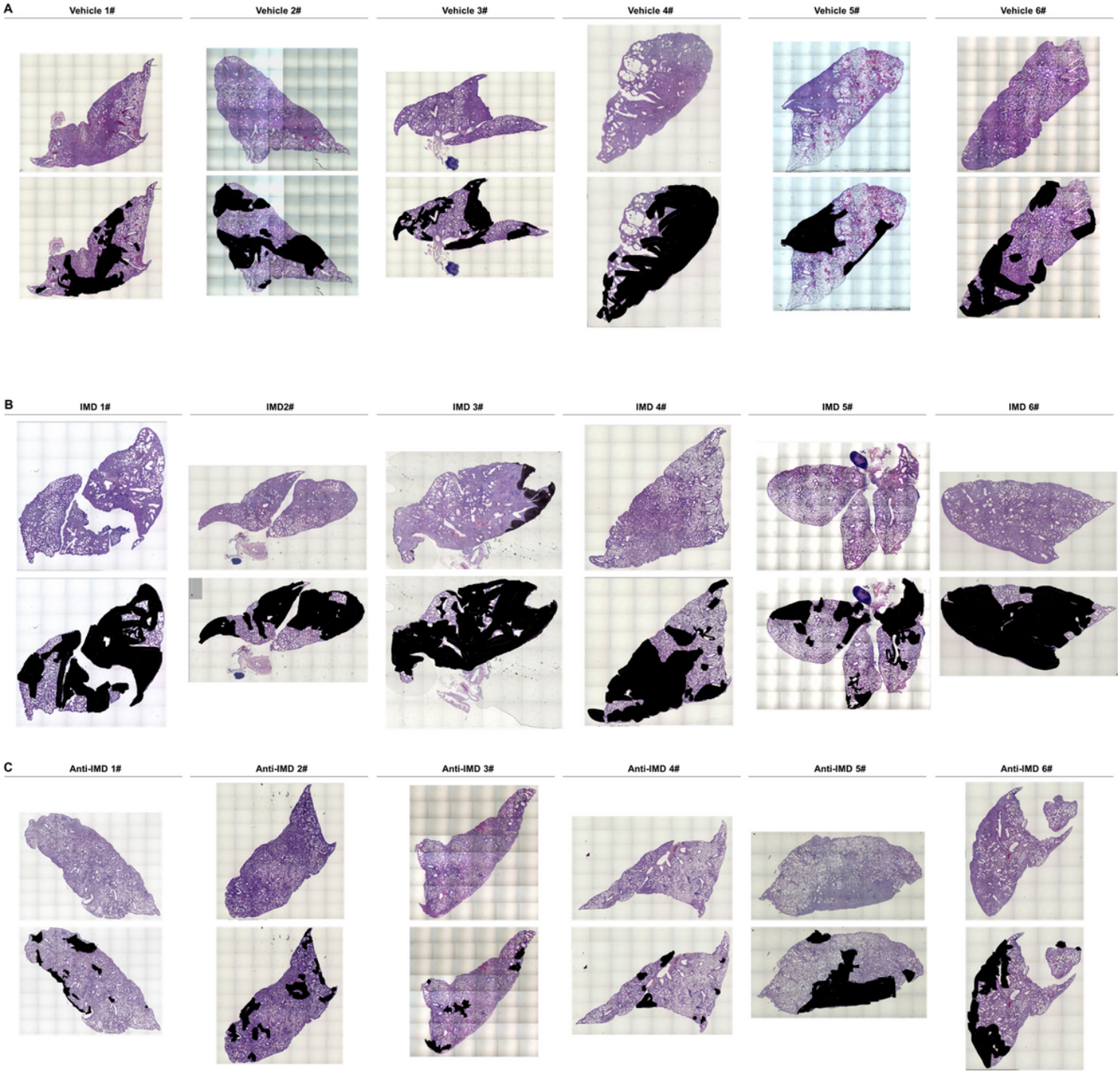

Figure 4

H&E staining of the whole lungs from the tumor-bearing mice. A-C, Five weeks after inoculation of 4T1 cancer cells, lungs from the tumor-bearing mice were removed, treated with 4% Paraformaldehyde for 24 hours, embedded in paraffin, and sliced for H&E staining. Upper panels: the whole pictures of the H&E-stained lungs. Lower panels: the metastatic tumor foci marked with pseudo-color (Black).

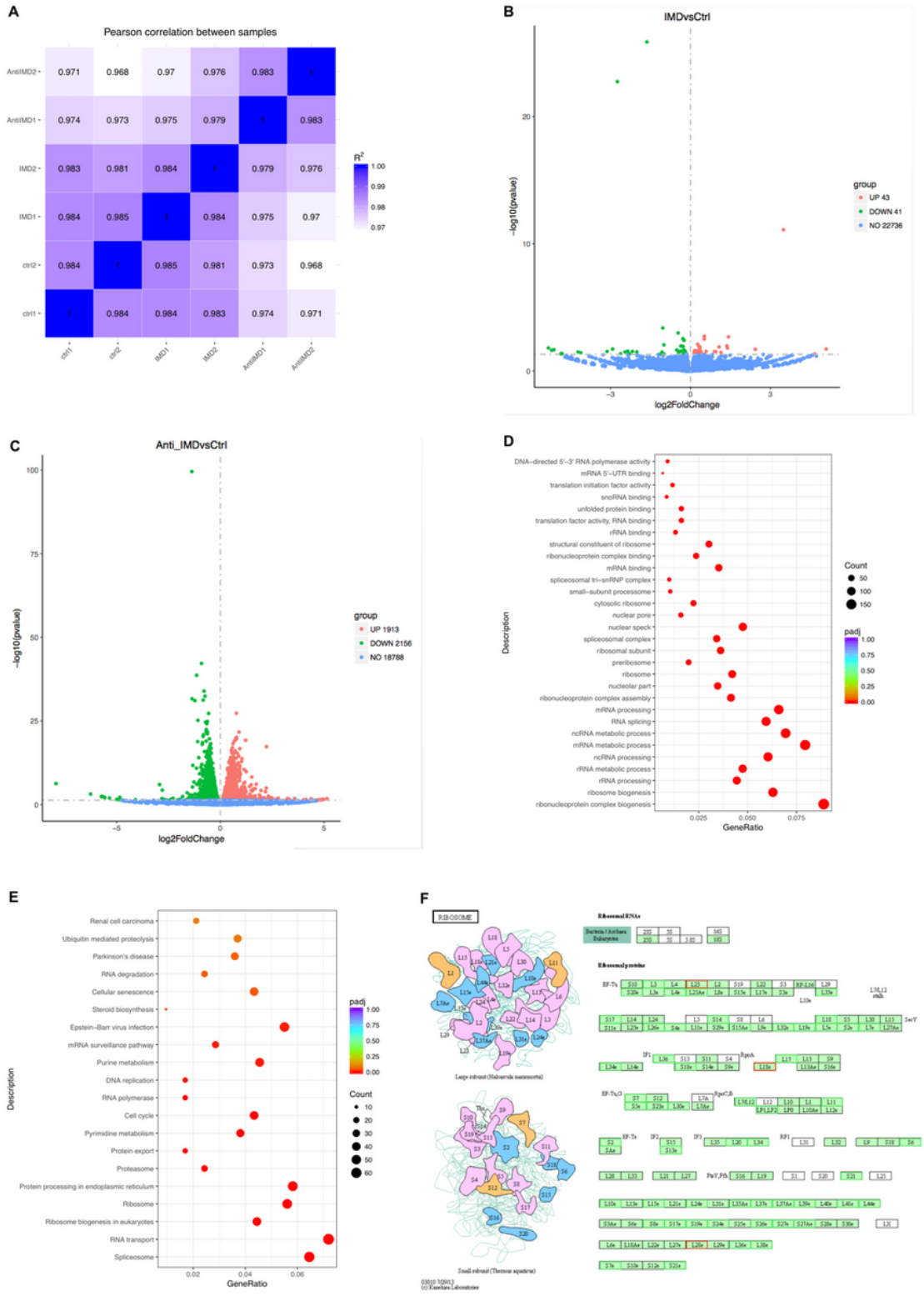

Figure 5

Blockade of IMD significantly inhibited ribosomal biogenesis and protein synthesis. A, The square of Pearson correlation coefficient (R2) of the RNA-Seq analysis. R2 > 0.92 indicates good reliability. B-C, Volcano graphs showed the distribution of differentially expressed genes for IMD vs. Ctrl and anti-IMD vs. Ctrl comparisons. D-E, GO and KEGG analysis showed that the anti-IMD antibody treatment had the greatest impact on ribosomal biogenesis and protein synthesis. F, The KEGG graphic analysis (KEGG term: Ribosome) showed that the anti-IMD antibody significantly reduced the transcription of the large and small subunits of ribosomes. The down-regulated genes were marked with green borders, and the up-regulated genes were marked with red borders.

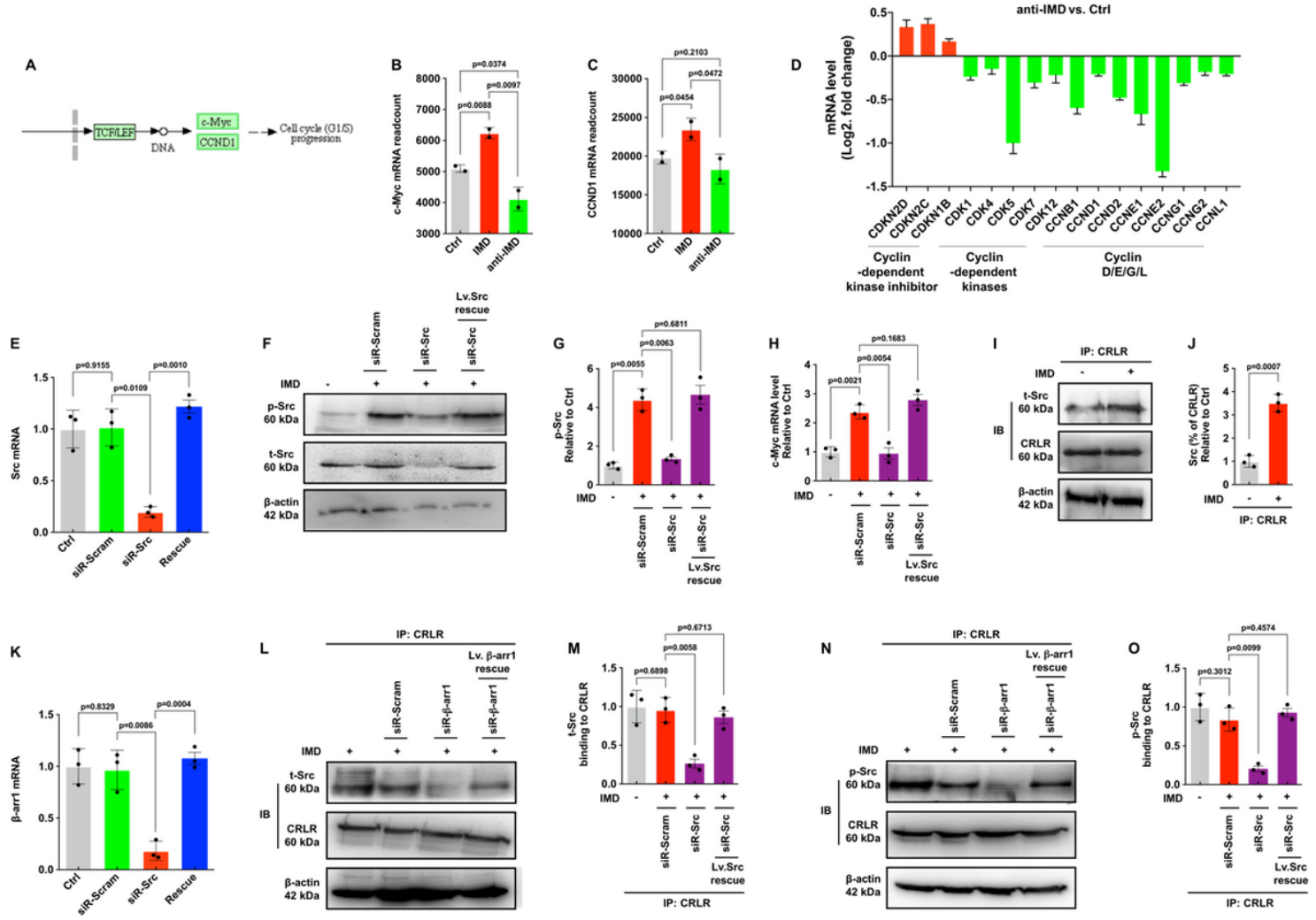

Figure 6

IMD activated a Src/c-Myc signaling pathway. A, The KEGG pathway analysis (KEGG term: Breast cancer) showed that treatment with the anti-IMD antibody suppressed the cell cycle (at the G1/S phase) by downregulating c-Myc and cyclin D1 (CCND1). Green borders marked the down-regulated c-Myc and CCND1. B-C: The RNA-Seq read counts of c-Myc and CCND1 genes from 4T1 cells treated with vehicle (PBS), IMD (2.5μg/ml), or the anti-IMD antibody (25μg/ml). D, The mRNA level changes (Log2. fold change) of cyclins, cyclin-dependent kinases, or cyclin-dependent kinase inhibitors after treatment of the anti-IMD antibody. Green bars indicate the down-regulated genes, and red bars indicate the up-regulated

genes. E, The mRNA level of Src in cell transfected with siR-Scram, siR-Src (or rescued by Lv.Src transfection). The mean value of control Src mRNA was set to 1.0, n=3. F, 4T1 cells transfected with siR-Scram, siR-Src (or rescued by Lv.Src transfection) were subjected to WB assay to detect Src phosphorylation. G, The density of the band for p-Src (referred to β-actin) is presented relative to that of the control. The mean level in the control group was set to 1.0; n=3. H, Level of c-Myc mRNA (relative to control) was calculated (n=3). I, 4T1 Cells were treated with IMD or vehicle for 10 min. Cell lysates were immunoprecipitated for CRLR and probed for total-Src and CRLR (as a reference). J, Density of the bands for co-precipitated proteins (relative to CRLR) were presented relative to that of the control, n=3. K, The mRNA level of β-arr1 in cell transfected with siR-Scram, siR-β-arr1 (or rescued by Lv.β-arr1 transfection), n=3. L and N, 4T1 Cells transfected with siR-Scram, siR-β-arr1 (or rescued by Lv.β-arr1 transfection) with the presence of IMD were immunoprecipitated for CRLR and probed for total-Src or phospho-Src and CRLR (as a reference). M and O, Density of the bands for co-precipitated proteins (relative to CRLR) were presented relative to that of the control; The mean level in the control group was set to 1.0; n=3. Data were presented with presented as scatter plots with mean ± SD. Significance was assessed by unpaired t test with Welch's correction.

Supplementary Files

This is a list of supplementary files associated with this preprint. Click to download.

- Additionalfile1.xlsx
- Additionalfile2.xlsx
- Additionalfile3.xlsx